New Phytologist

Research

N_2 fixation in free-floating filaments of *Trichodesmium* is higher than in transiently suboxic colony microenvironments

Meri Eichner[1], Silke Thoms[2], Björn Rost[2], Wiebke Mohr[1], Soeren Ahmerkamp[1], Helle Ploug[3], Marcel M. M. Kuypers[1] and Dirk de Beer[1]

[1]Max Planck Institute for Marine Microbiology, Celsiusstr. 1, Bremen 28359, Germany; [2]Alfred Wegener Institute, Helmholtz Centre for Polar and Marine Research, Am Handelshafen 12, Bremerhaven 27570, Germany; [3]Department of Marine Sciences, University of Gothenburg, Carl Skottbergsgata 22 B, Göteborg 41319, Sweden

Author for correspondence:
Meri Eichner
Tel: +49 421 2028 834
Email: meichner@mpi-bremen.de

Received: *2 August 2018*
Accepted: *22 November 2018*

New Phytologist (2018)
doi: 10.1111/nph.15621

Key words: colony, microenvironment, N_2 fixation, oxygen, *Trichodesmium*.

Summary

- To understand the role of micrometer-scale oxygen (O_2) gradients in facilitating dinitrogen (N_2) fixation, we characterized O_2 dynamics in the microenvironment around free-floating trichomes and colonies of *Trichodesmium erythraeum* IMS101.
- Diurnal and spatial variability in O_2 concentrations in the bulk medium, within colonies, along trichomes and within single cells were determined using O_2 optodes, microsensors and model calculations. Carbon (C) and N_2 fixation as well as O_2 evolution and uptake under different O_2 concentrations were analyzed by stable isotope incubations and membrane inlet mass spectrometry.
- We observed a pronounced diel rhythm in O_2 fluxes, with net O_2 evolution restricted to short periods in the morning and evening, and net O_2 uptake driven by dark respiration and light-dependent O_2 uptake during the major part of the light period. Remarkably, colonies showed lower N_2 fixation and C fixation rates than free-floating trichomes despite the long period of O_2 undersaturation in the colony microenvironment.
- Model calculations demonstrate that low permeability of the cell wall in combination with metabolic heterogeneity between single cells allows for anoxic intracellular conditions in colonies but also free-floating trichomes of *Trichodesmium*. Therefore, whereas colony formation must have benefits for *Trichodesmium*, it does not favor N_2 fixation.

Introduction

Fixation of dinitrogen (N_2) by marine diazotrophic bacteria and cyanobacteria provides a significant source of nitrogen to phytoplankton in oligotrophic systems. The N_2-fixing enzyme nitrogenase is inhibited by oxygen (O_2) via oxidative damage to the iron sulfur clusters (Burgess & Lowe, 1996), proteolysis (Durner *et al.*, 1996) as well as suppression of nitrogenase synthesis and posttranslational modification (Gallon, 1992). To protect nitrogenase from O_2, many single-celled cyanobacteria separate photosynthesis from N_2 fixation in time, conducting N_2 fixation during the night, whereas many filamentous cyanobacteria restrict N_2 fixation to specialized cells termed heterocysts. The genus *Trichodesmium* spp., a globally important, colony-forming diazotroph, is an exception in that it fixes N_2 during the day although it lacks heterocysts. A range of O_2-protective mechanisms has been suggested for *Trichodesmium*: the formation of anoxic microzones within colonies (Paerl & Bebout, 1988); a downregulation of photosynthesis during the peak of N_2 fixation at midday (Berman-Frank *et al.*, 2001); a restriction of N_2 fixation to specialized cells termed diazocytes (Bergman & Carpenter, 1991; Berman-Frank *et al.*, 2001); and dynamic switches between different photosynthetic activity states by reversible uncoupling of phycobilisomes from the photosystems on the time scale of minutes (Küpper *et al.*, 2004, 2009). The prevalence and coordination of these different mechanisms is still debated, partly due to conflicting results in previous studies.

Regarding cell specialization, several studies have reported nitrogenase to be present only in 10–15% of cells within a trichome (diazocytes), which are not terminally differentiated cells, do not have thicker cell walls than vegetative cells, and contain photosystem II, by contrast to heterocysts (Carpenter *et al.*, 1990; Siddiqui *et al.*, 1992a; Fredriksson & Bergman, 1995; Berman-Frank *et al.*, 2001). Other studies observed no differences in nitrogenase expression and/or N_2 fixation between single cells and therefore questioned the prevalence of diazocytes (Paerl & Bebout, 1988; Finzi-Hart *et al.*, 2009; Ohki & Taniuchi, 2009). Also the formation of anoxic microzones in colonies has been challenged by field measurements showing strong O_2 supersaturation in *Trichodesmium* colonies (Eichner *et al.*, 2017), questioning the assumed benefit of colony formation for N_2 fixation. Direct comparisons of colonies and single trichomes are scarce. Field studies have traditionally shown a bias towards studying colonies rather than single trichomes (Letelier & Karl, 1998), whereas most laboratory studies on *Trichodesmium* physiology, including those demonstrating the inhibitory effects of O_2 on N_2

fixation *in vivo* (Küpper *et al.*, 2004; Berman-Frank *et al.*, 2005, 2008; Staal *et al.*, 2007), have been conducted on cultures of *Trichodesmium erythraeum* IMS101 grown as single trichomes.

To re-evaluate the hypothesis that anoxic microenvironments allow for higher N_2 fixation in colonies compared with single trichomes, we conducted an in-depth analysis of O_2 dynamics and feedbacks on N_2 fixation in colonies and free-floating trichomes of *Trichodesmium erythraeum* IMS101. We directly compared carbon (C) and N_2 fixation rates in colonies vs single trichomes and characterized cellular gross and net O_2 fluxes, diurnal variations in O_2 concentrations in the bulk medium, and O_2 concentrations within colonies, on the surface of single trichomes and within single cells.

Materials and Methods

Culture conditions

Cultures of *Trichodesmium erythraeum* IMS101 were grown on YBCII culture medium (Chen *et al.*, 1996) with decreased phosphate concentrations (4.61 ± 0.79 µmol l^{-1}, determined with QuAAtro39, Seal Analytics), at 27–29°C and 240–280 µmol photons m^{-2} s^{-1} under a 12 h: 12 h, light : dark cycle. Stock cultures were grown on a shaking table (80 rounds min^{-1}, IKA KS 130 basic), and transferred to roller tanks once colonies had started to form in order to maintain colonies physically intact for longer. Additional colonies formed in roller tanks, including mostly puffs, but also tuft- and needle-shaped colonies. Depending on the culture volume required for the specific measurements, different roller tank set-ups were used, including bottles with a volume between 60 ml and 2.5 l. pH levels (National Bureau of Standards (NBS) scale) were determined with a two-point calibrated glass electrode (Aquatrode plus Pt1000; Metrohm, Herisau, Switzerland).

Elemental composition

For determination of elemental ratios, samples for particulate organic carbon, nitrogen and phosphorus (POC, PON and POP) and chlorophyll *a* (Chl*a*) were taken *c.* 7 h after beginning of the light phase. Technical duplicate samples of culture including both free trichomes and colonies were filtered onto precombusted GF/F filters and stored at −20°C. Samples for analysis of POC and PON were acidified with 200 µl HCl (0.2 mol l^{-1}) and subsequently measured on an elemental analyzer (EuroEA, Eurovector). POP was determined spectrophotometrically (UV-1202; Schimadzu, Kyoto, Japan) according to Hansen & Koroleff (1999). Chl*a* was extracted in 90% acetone at 4°C for > 12 h with ultrasonication (10 s) and measured fluorometrically (10-AU, Turner Designs; Holm-Hansen & Riemann, 1978).

Optode measurements

The diurnal cycle of O_2 concentrations in cultures was monitored with contactless optical O_2 sensors glued into culture vessels (silicon glue, sensor spots of 5 mm diameter and a FireStingO2/FireStingGO2 oxygen meter, Pyroscience). Measurements were performed in 120 ml serum bottles closed without headspace and incubated in roller tanks. Additionally, O_2 concentrations were monitored in the set-up used for stock cultures, that is, culture vials closed with a gas permeable frit (VWR) that were incubated on a shaking table. O_2 concentrations were recorded at 2 Hz for up to 7 d. Optodes were two-point calibrated using medium that was bubbled with either N_2 gas or air to achieve 0% and 100% air saturation, respectively.

Microsensor measurements

Microsensor measurements on colonies were performed in a custom-made flow system (Ploug & Jørgensen, 1999) in YBCII medium at 26°C. Single colonies were suspended in the flow chamber (flow < 0.1 mm s^{-1}), fixed with a thin glass needle and observed through a stereomicroscope (Stemi SV6; Zeiss). For recording depth profiles through the colony center, microsensors were moved towards and into the colony with a motor-driven micromanipulator (VT-80, Micos/Faulhaber Minimotor SA).

In a total of 13 colonies, O_2 concentrations in and around colonies were measured with Clark-type microelectrodes (tip diameter *c.* 10–15 µm, response time *c.* 1 s). Rates of respiration and net photosynthesis were calculated from the steady-state O_2 gradient at the colony surface according to Fick's first law of diffusion:

$$J = -D(\Delta C/\Delta r),$$

where J represents the interfacial O_2 flux, D the diffusion coefficient for O_2 (2.26×10^{-9} m^2 s^{-1} at 25°C and salinity 34; Broecker & Peng, 1974), and ΔC the concentration difference measured over the respective distance, Δr, at the colony surface. Surface area and volume were determined for each colony assuming ellipsoid geometry and used to convert interfacial flux to volume-normalized rates. The theoretical maximum O_2 uptake supported by diffusive O_2 supply (that is, the O_2 uptake rate yielding anoxia at the center of the colony) was calculated as a function of colony volume as described by Ploug *et al.* (1997). An apparent diffusivity of O_2 within the colony of 0.95× that of seawater, a Sherwood number of 1 (that is, no difference between the motion of the colony and that of the surrounding water, resulting in mass transfer merely by molecular diffusion but not advection), a bulk O_2 concentration of 212 µmol l^{-1} (that is, air saturation), and a uniform respiration rate throughout the colony were assumed.

Additionally, measurements of chlorophyll fluorescence were performed on nine of the colonies using a MicrofiberPAM (Walz) with a microfiber tapered to 10–20 µm width at the tip. A red LED (650 nm) was used for excitation. Measurements were performed in the dark, between 1 and 9 h after beginning of the light phase. Photochemical quantum yield (F_v/F_m) is reported only for those positions in and around colonies for which signal strength was high enough for a clear fluorescence induction curve to be observed.

For microsensor measurements on single trichomes with higher spatial resolution, the trichomes were embedded in 0.5%

agar, in which the effective diffusion coefficient of O_2 is similar as in seawater (Ploug & Passow, 2007). Ultra-pure low melting point agar (Invitrogen) was dissolved, allowed to cool down to < 30°C, and then mixed in a ratio of *c.* 1 : 1 with culture in a Petri dish. Measurements were performed on a total of 29 trichomes with Clark-type microelectrodes (tip diameter 5–10 µm, response time *c.* 1 s) under an inverted microscope (Axiovert 25; Zeiss) at ×20 magnification, room temperature and *c.* 150 µmol photons m^{-2} s^{-1} (unless specified otherwise), at various time points between the start and 1 h after the end of the light period. Differences in O_2 concentrations along trichomes were probed by moving the sensor along the trichome within *c.* 3 µm distance from the cell surface as observed in the microscope, and recording O_2 concentrations in consecutive steps of three to four cells. Additionally, O_2 concentrations were recorded continuously at the surface of individual cells while switching the light on and off.

Membrane inlet mass spectrometry

Gross and net O_2 fluxes were measured with a custom-built membrane inlet mass spectrometer (MIMS; mass spectrometer Isoprime, custom-built 8 ml cuvette) using the $^{18}O_2$-based approach described by Fock & Sültemeyer (1989). Cultures containing colonies and single trichomes were grown in 2.5 l Schott bottles at 25°C and 300 µmol photons m^{-2} s^{-1} (Biolux; Osram, Garching, Germany). For measurements, $^{18}O_2$ gas (Chemotrade, Düsseldorf, Germany) was dissolved in previously N_2-bubbled YBCII medium buffered with HEPES (50 mmol l^{-1}, pH 8.29 ± 0.06), reaching a final concentration of *c.* 150% air saturation. Cultures concentrated by gentle filtration over a polycarbonate filter, as well as additional colonies picked with a Pasteur pipette, were suspended in the $^{18}O_2$-enriched medium, reaching a final Chl*a* concentration of 0.41 ± 0.26 µg ml^{-1}. The production of $^{16}O_2$ and the uptake of $^{16}O_2$ and $^{18}O_2$ were then monitored in light and dark under three different O_2 concentrations (346 ± 39 µmol l^{-1}, 191 ± 51 µmol l^{-1} and 101 ± 35 µmol l^{-1}) obtained by bubbling with N_2 gas. Samples were stirred during measurements, resulting in disassembly of the colonies. Two replicate light and dark phases lasting *c.* 4 min each were conducted at each O_2 level. O_2 signals were corrected for abiotic consumption and influx of O_2 into the cuvette by subtracting O_2 slopes recorded in abiotic controls at the respective O_2 concentrations. In total, 11 samples containing free-floating trichomes and colonies in various proportions were analyzed. Measurements were performed between 1.5 and 4 h after the beginning of the light phase (except one measurement at 8–9 h after the beginning of the light phase that yielded results that were not different from the others).

Stable isotope incubations

C and N_2 fixation rates of free-floating trichomes and colonies were determined by stable isotope incubations with $NaH^{13}CO_3$ (Sigma Aldrich) and $^{15}N_2$ gas (Cambridge Isotope Laboratories, Tewksbury, MA, USA). To ensure dissolution of $^{15}N_2$ gas, $^{15}N_2$ and $NaH^{13}CO_3$ were predissolved in YBCII medium for > 12 h before incubations. Final enrichment was 3.44 ± 0.24 atom percent excess (at% excess) for ^{13}C and 2.2 ± 1.06 at% excess for ^{15}N, as determined at the end of incubations for each incubation bottle by cavity ring-down spectroscopy (G2201-i; Picarro, Santa Clara, CA, USA) and MIMS (GAM2000; InProcess, Bremen, Germany). O_2 concentrations in the incubation medium were adjusted to low (24 ± 11 µmol l^{-1}), ambient (238 ± 13 µmol l^{-1}) or high (475 ± 32 µmol l^{-1}) levels by bubbling with a mixture of helium and N_2 (20% : 80%, low O_2 treatment), room air (ambient O_2 treatment), or a mixture of O_2 and N_2 (40% : 60%, high O_2 treatment). Subsequently, *Trichodesmium* biomass was transferred to the respective medium and amended with ^{15}N- and ^{13}C-enriched stock solutions. For incubations of colonies, approx. 50 colonies per incubation vial were picked from culture bottles with a Pasteur pipette. For incubations of free-floating trichomes, the remaining culture volume was concentrated by filtration over a polycarbonate filter before transfer to the incubation medium. Samples where free-floating trichomes formed colonies during the incubation period, resulting in colony-dominated biomass, were classified as colonies. Incubations were performed in triplicate, in 60 ml serum vials at 25°C and 150 µmol photons m^{-2} s^{-1} (100–210 µmol photons m^{-2} s^{-1} in roller tanks), for 11 h starting within 1 h after beginning of the light period. The O_2 concentration in each incubation vial was measured with O_2 microsensors before and after incubations. Vials with single trichomes were gently agitated by hand *c.* 4 times over the incubation period. Vials with colonies were incubated in roller tanks. At the end of the incubation time, cultures were filtered on precombusted GF/F filters and stored at −20°C. Before analysis, filters were acidified in an HCl fume (overnight) to remove all inorganic carbon. Amounts of POC and PON and their isotopic composition were measured by elemental analyser isotope ratio mass spectrometry (EA-IRMS, Delta Plus XP and Flash EA 112; Thermo Fisher Scientific, Waltham, MA, USA). ^{13}C and ^{15}N enrichment of the POC and PON relative to the bulk solution was then converted to C and N_2 fixation rates normalized to cellular C and N biomass, respectively, yielding C- and N-specific fixation rates. The dissolved inorganic carbon concentration in incubation vials at the end of the incubation period was never below 1820 µmol l^{-1}.

Results

Culture characteristics

Single trichomes and colonies co-occurred in the cultures in varying proportions. Cultures generally started forming colonies 1 wk or longer after dilution with fresh medium and stayed in a colony-dominated state for more than a week. Colonies were often formed in high numbers within a short time period, starting with needle- or string-shaped colonies that formed around 200 mostly puff-shaped colonies l^{-1} within a day, which were morphologically similar to field-collected puffs. Continuous monitoring of bulk O_2 concentrations within culture vials over

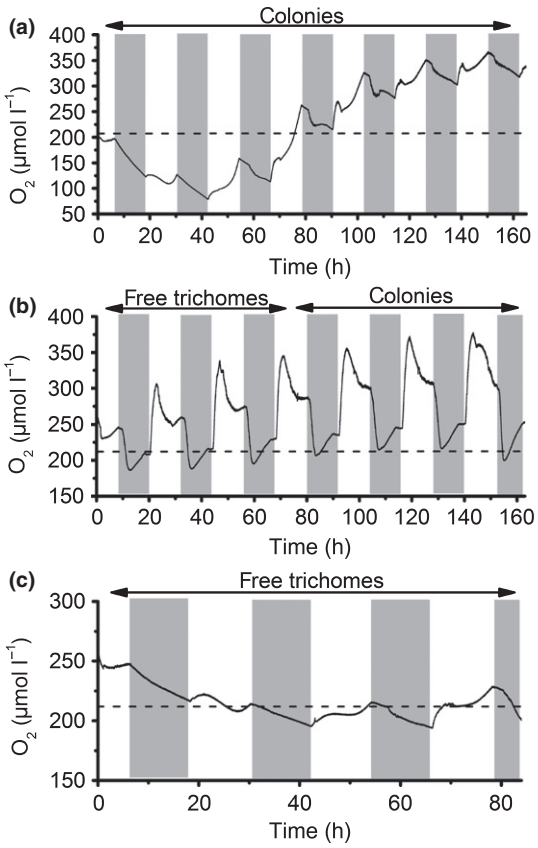

Fig. 1 O_2 concentrations in the bulk medium of *Trichodesmium* cultures incubated in roller tanks, monitored in three replicate vials (a–c). Dominant morphology (free-floating trichomes or colonies) is indicated above each panel. Note that total biomass differed between vials and changed over time. Dashed lines indicate O_2 concentration at air saturation, and grey shaded areas indicate dark phases (that is, night-time).

several days showed that the cultures were net phototrophic most of the time (Fig. 1). This trend was independent of the relative abundance of colonies vs single trichomes, that is, no changes were observed once cultures went from a single-trichome- to a colony-dominated state (Fig. 1b). Key characteristics of the cultures are summarized in Table 1. pH levels were higher in cultures than in abiotic reference medium (*t*-test, $P < 0.005$, Table 1), confirming net phototrophic growth. Monitoring of phosphate concentrations in two representative bottles over 8 d showed phosphate consumption. Elemental ratios in biomass were variable, with average values close to the Redfield ratio. POC : PON ratios in samples taken from stable isotope incubations at the end of the light period were higher than those taken *c.* 7 h after the beginning of the light period, and showed no significant difference between colonies and trichomes (*t*-test, $P > 0.05$, Table 1).

Diel variation in bulk O_2 concentrations

Continuous measurements of O_2 concentrations in the culture medium revealed strong variations over the diel cycle, both in closed vials (Fig. 1), and in culture flasks with a gas permeable lid (up to 300 µmol l^{-1}; data not shown). Often, a fast rise in O_2 concentrations was observed within a short period of 1–3 h in the morning, followed by a slow decrease in O_2 concentrations over several hours (Fig. 1). A second phase of net O_2 evolution followed in most cases 2–4 h before the beginning of the dark phase. Net O_2 evolution over the 12 h light period ranged between −3 µmol l^{-1} (12 h)$^{-1}$ (that is, net O_2 consumption) and 146 µmol l^{-1} (12 h)$^{-1}$. During the night, a net decrease of O_2 concentrations was observed, sometimes including a short and steep decrease during the first hours of the night. Remarkably, this initial decrease was followed by an increase to air saturation level or above, while the incubation was still in the dark (Fig. 1b). This pattern was confirmed by tracking O_2 concentrations close to the center of single colonies with microsensors over several hours (Supporting Information Fig. S1b,d). In the morning, maximum O_2 concentrations of 570 and 326 µmol l^{-1} were observed within colonies (0.5 and 1.3 h after beginning of the light period, respectively; Fig. S1a,c). In the evening, three out of six colonies examined showed elevated O_2 concentrations (e.g. 450 µmol l^{-1} measured 2 h before the beginning of the dark period, Figs 2d, S1). During most of the day, however, colonies were undersaturated with O_2 (Fig. 2a–c) and net photosynthesis calculated from O_2 profiles was negative (Fig. 2e). To shed light on the regulation of O_2 concentrations specifically during this phase of O_2 undersaturation, O_2 microenvironments and cellular gross and net O_2 fluxes were analyzed in more detail during the middle of the day.

Table 1 Key characteristics of *Trichodesmium* cultures used in the experiment (mean ± SD).

pH in culture medium		8.52 ± 0.06	$n = 7$
pH in abiotic reference medium		8.38 ± 0.06	$n = 9$
Phosphate uptake (replicate 1)	µmol l^{-1} d^{-1}	0.08	
Phosphate uptake (replicate 2)	µmol l^{-1} d^{-1}	0.12	
F_v/F_m[†]		0.46 ± 0.07	$n = 9$
POC : PON (7 h)[‡]	mol mol^{-1}	5.5 ± 1.2	$n = 4$
POC : PON (12 h)[§]	mol mol^{-1}	8.3 ± 2.6	$n = 28$
POC : POP[‡]	mol mol^{-1}	100 ± 75	$n = 4$
PON : POP[‡]	mol mol^{-1}	20 ± 16	$n = 4$
POC : chlorophyll *a*[‡]	µg $µg^{-1}$	256 ± 116	$n = 3$

F_v/F_m, photochemical quantum yield; POC, particulate organic carbon; PON, particulate organic nitrogen; POP, particulate organic phosphorus.
[†]Measured along transects across individual colonies.
[‡]Bulk culture samples taken 7 h after beginning of the photoperiod.
[§]Samples taken at the end of the photoperiod, average value including colonies and single trichomes incubated under different O_2 concentrations.

O_2 microenvironments in colonies during the middle of the day

O_2 profiles were measured on a total of 13 colonies of different size (250–1500 µm diameter), shape (tufts and puffs), buoyancy and trichome density between 0.45 and 8 h after beginning of the light period, that is, covering the time period of decreasing O_2 evolution rates in the bulk medium (Fig. 1). O_2 concentrations in the center of the colony ranged from anoxic conditions to close to air saturation (Fig. 2a–c). Net O_2 uptake rates ranged from 0.02 to 26.5 nmol colony^{-1} h^{-1}. O_2 uptake in light was

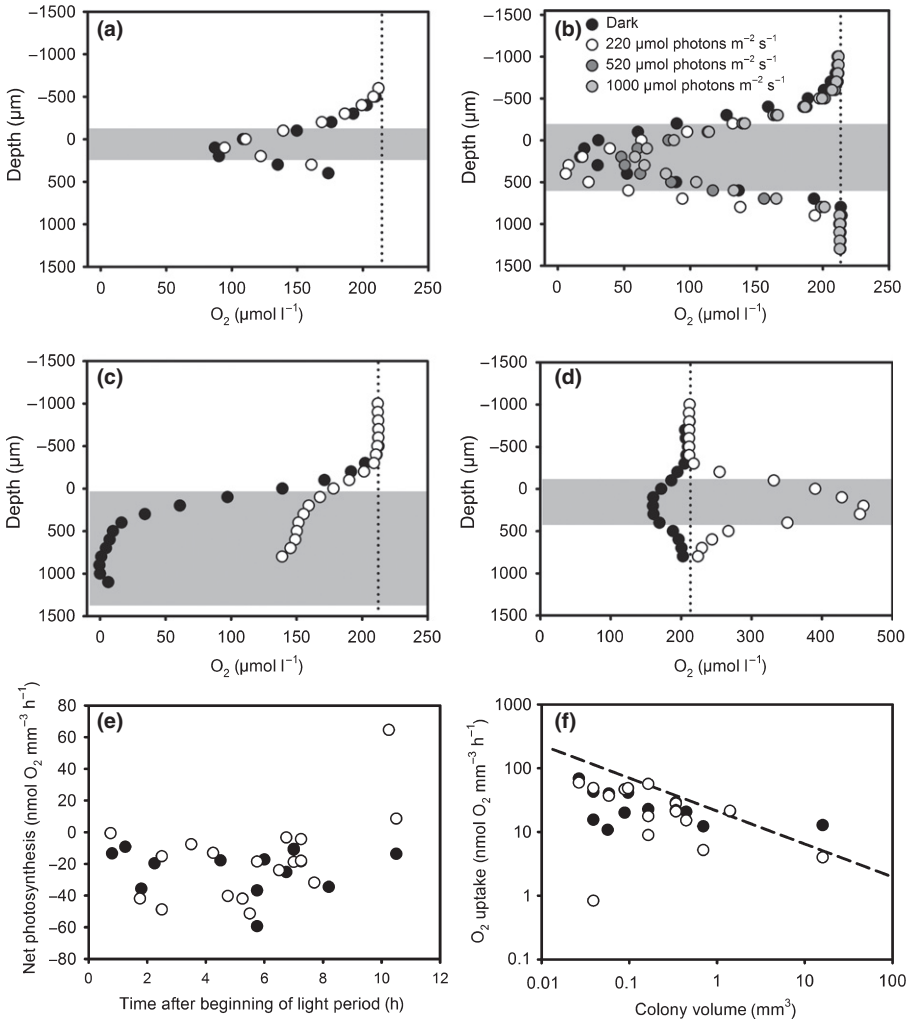

Fig. 2 (a–d) Examples of O_2 profiles measured in *Trichodesmium* colonies of different sizes (a, 0.02 mm^3; b, 0.38 mm^3; c, 2.4 mm^3; d, 0.16 mm^3) at different light intensities and times of the day (a, 6 h; b, 6 h; c, 7 h; d, 10 h, after the beginning of the light phase). Note the different scale of *x*-axis. Grey shading indicates approximate position of the colony, dotted lines indicate O_2 concentration at air saturation. (e) Net photosynthesis rates calculated from depth profiles through colonies measured at different times of the day. (f) Net O_2 uptake by colonies in dependence of colony volume. Dashed line indicates diffusion limitation (calculated according to Ploug *et al.*, 1997).

correlated to dark respiration with an R^2 of 0.699 (linear regression). Volume-normalized O_2 uptake was not significantly affected by light intensity (*t*-test, $P > 0.05$; Table 2) and colonies undersaturated with O_2 were observed under light intensities up to 1000 µmol photons m^{-2} s^{-1} (Fig. 2b). A comparison of the measured O_2 uptake rates with calculated O_2 diffusion rates into the colony revealed that O_2 uptake in both light and dark ranged up to the predicted maximum rate allowed by diffusive O_2 supply (Fig. 2f). Measurements of chlorophyll fluorescence did not show any spatial patterns of photosynthetic activity along colony transects (data not shown).

Table 2 Net O_2 uptake rates (mean ± SD) by *Trichodesmium* colonies based on O_2 profiles measured at different light intensities at 45 min to 8 h after beginning of the light period.

Light intensity µmol photons m^{-2} s^{-1}	Net O_2 uptake		
	nmol O_2 colony^{-1} h^{-1}	nmol mm^{-3} h^{-1}	
Dark	4.0 ± 6.8	23 ± 14	$n = 14$
200	2.4 ± 2.3	24 ± 17	$n = 16$
500	1.4 ± 1.8	13 ± 8	$n = 8$
1000	3.1 ± 3.4	15 ± 1	$n = 2$

Cellular O_2 fluxes during the middle of the day

Measurements of O_2 fluxes in colonies and single trichomes during late morning/midday using an $^{18}O_2$-based MIMS approach yielded net O_2 production rates that were often close to zero or negative (Fig. 3), in line with microsensor measurements performed during this part of the day (Fig. 2). The low net photosynthesis was a result of 4–5 times higher gross O_2 uptake balancing gross O_2 evolution. Dark respiration and light-dependent O_2 uptake (e.g. classical Mehler reaction and/or flavoprotein-mediated O_2 uptake) amounted to 56 ± 31% and 42 ± 63% of gross O_2 evolution, respectively. Measurements under different external O_2 concentrations mimicking the range observed in the center of colonies (e.g. Fig. 2) showed that gross O_2 evolution, dark respiration, and light-dependent O_2 uptake increased with increasing external O_2 concentration, whereas net photosynthesis decreased (analysis of variance (ANOVA), $P < 0.05$; Fig. 3) and was always negative when O_2 concentrations above air saturation were applied. Test measurements revealed that these effects of elevated O_2 levels were reversible; for

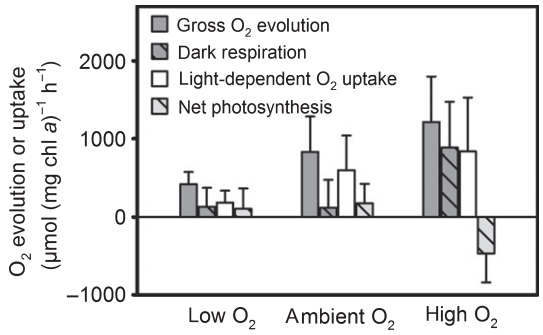

Fig. 3 O_2 production and uptake rates in *Trichodesmium* cultures measured during late morning/midday under different external O_2 concentrations. Cultures contained both colonies and free trichomes. Note that positive values on the *y*-axis indicate rates of both O_2 evolving and O_2 consuming processes. Light-dependent O_2 uptake is the difference between total O_2 uptake measured in the light and total O_2 uptake measured in the dark. Low O_2, 101 ± 35 μmol l^{-1}; ambient O_2, 191 ± 51 μmol l^{-1}; high O_2, 346 ± 39 μmol l^{-1}. $n = 11$ for low and ambient O_2, $n = 7$ for high O_2. Error bars ± SD.

instance, gross O_2 evolution measured under ambient O_2 was not significantly affected by O_2 concentration in the preceding light phase (*t*-test, $P > 0.05$, $n \geq 4$; data not shown). The relative amount of colonies and free-floating trichomes did not have consistent effects on O_2 fluxes, with higher dark respiration in colonies than free trichomes observed only under ambient O_2 (*t*-test, $P < 0.05$, $n \geq 4$) and higher total O_2 uptake in colonies observed only under low O_2 (*t*-test, $P < 0.05$, $n \geq 4$).

O_2 on the surface of single trichomes

To analyze variability at the level of single cells, O_2 concentrations on the surface of single trichomes were measured with microsensors at a spatial resolution equivalent to *c.* 2–4 cells (Fig. 4). O_2 concentrations on the surface of single trichomes as well as in the surrounding agar never deviated more than *c.* 30 μmol l^{-1} from air saturation level. Changes in O_2 concentrations on the cell surface when switching between light and dark ranged between 1 and 8 μmol l^{-1} (2.8 ± 1.8 μmol l^{-1}, recorded in 27 measurements on a total of nine filaments; examples given in Fig. 4a–c). To test comparability of results from this set-up with those obtained on colonies in the flow system, O_2 concentrations were measured on the surface of a trichome located in the periphery of a tuft-shaped colony, yielding a deviation in light vs dark of 70 μmol l^{-1} (data not shown). In the light, O_2 concentrations on the trichome surface differed by up to 6 μmol l^{-1} between cells/regions within a single trichome (Fig. 4d–f). Distinct areas with lower than average O_2 concentrations were observed in 11 out of the 26 trichomes analyzed. These areas were between 10 and 50 cells long and often located in the middle of trichomes.

Effects of O_2 concentrations on C and N_2 fixation

N_2 fixation was strongly O_2-dependent, with a clear inhibition in treatments with air-saturated medium and medium containing elevated O_2 concentrations compared to medium undersaturated in O_2 (two-way ANOVA and Holm-Sidak test, $P < 0.05$; Fig. 5a). At low O_2 concentrations, representative for minimum O_2 levels observed in the colony center (e.g. Fig. 2), N_2 fixation was increased by a factor of up to 4 compared to ambient O_2 concentrations (Fig. 5a). At elevated O_2 concentrations, representative for maximum O_2 levels observed in the colony center (e.g. Fig. 2), N_2 fixation rates were close to zero (Fig. 5a). Colonies showed lower N_2 fixation rates than free-floating trichomes (two-way ANOVA, $P < 0.05$; Fig. 5a). Pair-wise comparison under each O_2 level showed that this effect was only significant under low O_2 (Holm−Sidak test, $P < 0.05$). Similarly, colonies also showed lower C fixation rates than free-floating trichomes (two-way ANOVA, $P < 0.05$; Fig. 5b), with pair-wise comparison showing a significant difference only under low O_2 (Holm-Sidak test, $P < 0.05$). C fixation was not significantly affected by the O_2 treatment (two-way ANOVA, $P > 0.05$). C-specific O_2 evolution was not significantly affected by the O_2 treatment and was not different between colonies and free-floating trichomes (two-way ANOVA, $P > 0.05$; Fig. 5c).

Discussion

Physiological state of the cultures

Several observations indicate net biomass production in the colony-forming cultures in this study. Firstly, the increases in pH and phosphate consumption in the medium demonstrate that the cultures were growing (Table 1). Although brief net heterotrophic phases were observed (e.g. first day in Fig. 1a,c), which could potentially be sustained by uptake of dissolved organic matter accumulated in the medium (Benavides *et al.*, 2017), O_2 concentrations generally increased over the duration of several days, confirming net autotrophy (Fig. 1). Both free-floating trichomes and colonies were able to significantly increase N_2 fixation rates within a day when exposed to reduced O_2 concentrations (Fig. 5a). Colonies formed during the 12 h incubation period had similar N_2 fixation rates as older colonies (data not shown), indicating that 'old' colonies were not in a senescent state. These findings are in contrast with a previous report attributing low N_2 fixation rates in colonies of *Trichodesmium* NIBB 1067 to colony formation only during stationary growth phase (Ohki & Fujita, 1988).

C : N and C : Chl*a* ratios in particulate organic matter as well as C and N_2 fixation rates were in a similar order of magnitude as previous data on field-collected *Trichodesmium* colonies (Letelier & Karl, 1998; Eichner *et al.*, 2017). POC : POP ratios were lower than those previously measured in the field (Letelier & Karl, 1998; Orcutt *et al.*, 2013), and similar to P-replete cultures of *Trichodesmium* IMS101 (Spungin *et al.*, 2014), indicating that our cultures were not P-limited. F_v/F_m, a general indicator for the health status of photosynthetic organisms that is often used to detect iron (Fe) limitation, was higher in our study than previous measurements on free-floating, exponentially growing trichomes of the same strain (0.44 ± 0.11 (our study) vs 0.18–0.35 (Eichner *et al.*, 2014; measured with a blue LED)), suggesting that colonies were not stressed or severely Fe-depleted. By contrast with a recent laboratory study by Tzubari *et al.* (2018), we

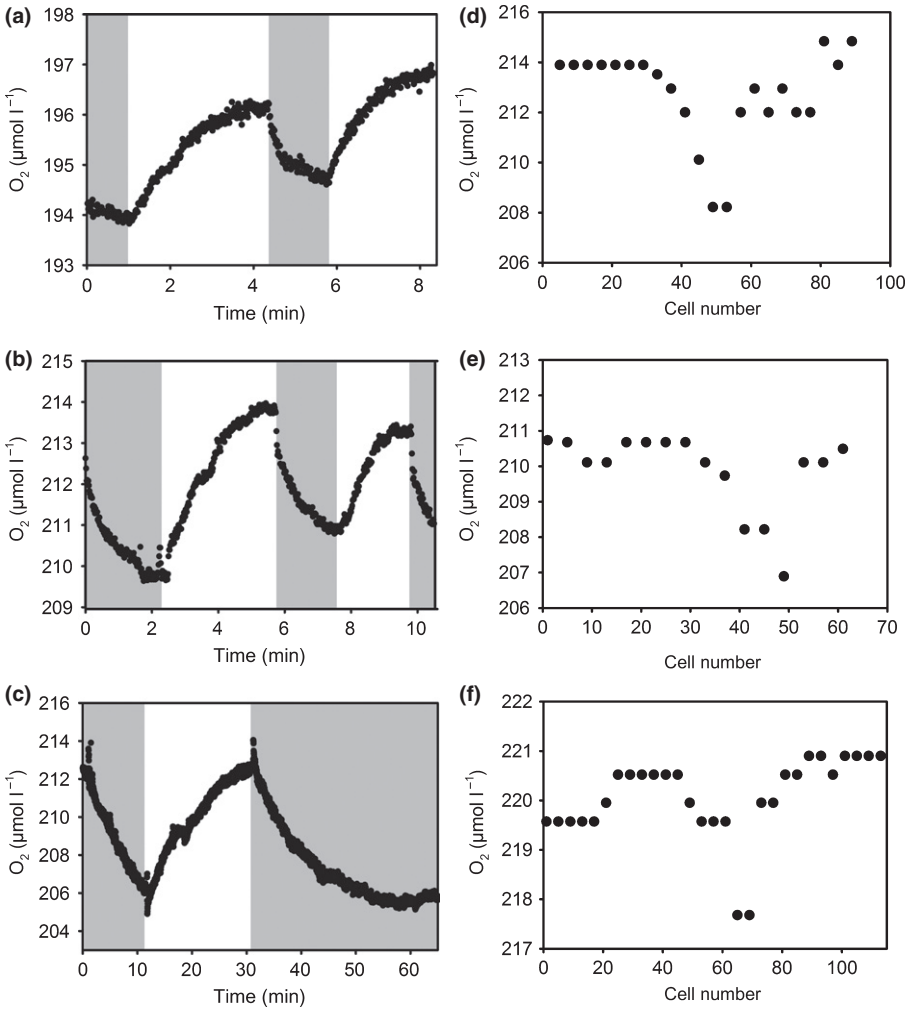

Fig. 4 Examples of O_2 concentrations measured within *c*. 3 µm of the surface of single *Trichodesmium* filaments during consecutive light and dark phases (a–c) and while sliding along the trichome with a microsensor (d–f; total duration of the measurement *c*. 20 min). Grey shaded areas indicate dark phases.

therefore assumed that, in our experiment, colony formation was not induced by P- or Fe-depletion. As we did not observe any differences in abiotic conditions or cellular composition between free-floating trichomes and colonies, the triggers for colony formation could not be identified. As cultures were grown under the same (*macro*scale) conditions, we relate the observed physiological differences to microenvironments within colonies.

Variation over the diel cycle

The downregulation of net photosynthesis during the middle of the day (Figs 1, 2e) is in line with previous observations on *Trichodesmium* in the field and laboratory (Berman-Frank *et al.*, 2001; Eichner *et al.*, 2014) and coincides with the peak in N_2 fixation observed 4–5 h after the beginning of the light period in *Trichodesmium* IMS101 (e.g. Kranz *et al.*, 2010; Eichner *et al.*, 2014). The switch from N_2 fixation back to photosynthesis in the afternoon was also reflected in higher POC : PON ratios measured at the end of the light period compared with the afternoon (Table 1), in line with previous observations (Kranz *et al.*, 2009). The magnitude of diel variations in O_2 was exceptionally large, reaching net O_2 uptake during the middle of the day (Figs 1, 2e), whereas previous studies merely showed a reduction of net O_2 evolution by 40–70% (Berman-Frank *et al.*, 2001; Eichner *et al.*, 2014). To understand the physiological mechanisms leading to this net O_2 uptake during the N_2 fixation phase, we investigated gross O_2 fluxes in this period by MIMS.

These measurements revealed a high ratio of gross to net O_2 evolution comparable with previous field observations on *Trichodesmium* (e.g. Kana, 1993), and exceeding previous estimates for free-floating trichomes of *Trichodesmium* IMS101 under comparable conditions (Kranz *et al.*, 2010; Eichner *et al.*, 2014). Such high O_2 uptake suggests that *Trichodesmium* decreases O_2 concentrations during the day by an upregulation of O_2-consuming processes such as dark respiration, classical Mehler reaction and/or flavoprotein-mediated O_2 uptake, rather than a downregulation of O_2 evolution. This way, electron transport through the photosynthetic and respiratory transport chain, and therefore proton translocation, is maintained even through the phase of low net O_2 production. This may serve as a means to maintain the production of ATP to support N_2 fixation, and is also in line with the relatively high F_v/F_m observed at the same time (Table 1). While O_2 uptake by Mehler reaction does not involve carbon fluxes, the high dark respiration rates observed here require the breakdown of a significant amount of carbohydrates produced in the preceding morning hours. For instance,

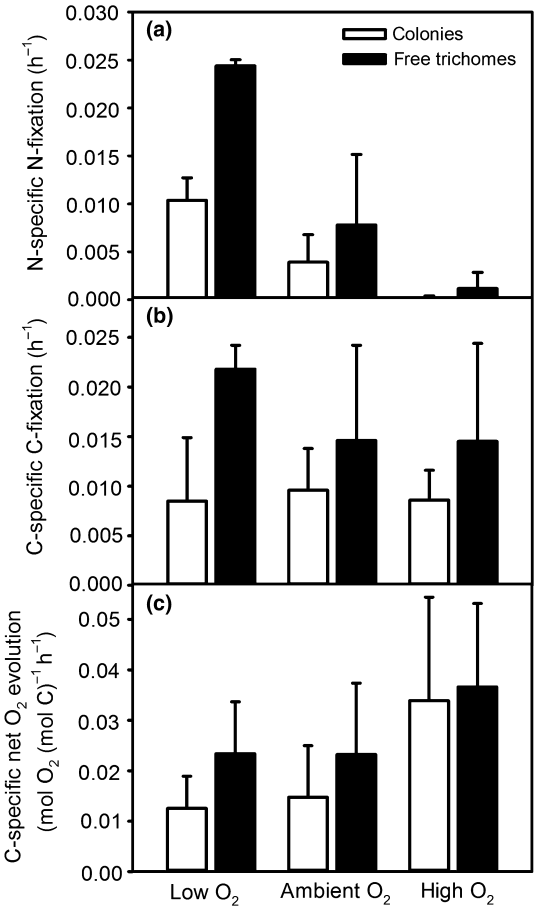

Fig. 5 (a) N_2 fixation, (b) C fixation and (c) O_2 evolution in free-floating trichomes and colonies of *Trichodesmium* measured under different O_2 concentrations in the bulk medium over the duration of the light phase (12 h). Low O_2, 24 ± 11 μmol l^{-1}; ambient O_2, 238 ± 13 μmol l^{-1}; high O_2, 475 ± 32 μmol l^{-1}. $n \geq 3$, except for trichomes at low O_2 with $n = 2$ in (a, b), and colonies at high O_2 with $n = 2$ in (c). Error bars indicate SD.

maintaining the dark respiration rates observed at high O_2 concentrations (Fig. 3) for 7 h would consume *c.* 30% of the POC at a typical cell density observed in our cultures (200 μmol C l^{-1}). In *Crocosphaera*, a similar diel cycle including the build-up of carbohydrates during the day and their breakdown at night has been proposed to support the high energy demand related to protecting nitrogenase under ambient O_2 levels (Großkopf & LaRoche, 2012). In *Trichodesmium*, energy and carbon budgets may differ substantially on a single-cell level due to cell specialization, depending on how diazocytes acquire carbohydrates and/or energy equivalents to support respiration and N_2 fixation. As the downregulation of net photosynthesis under elevated O_2 observed during MIMS measurements in the late morning (Fig. 3) was not observed in 12 h incubations (Fig. 5c), it seems to be a transient effect that is outbalanced on a diurnal time scale. It might represent a regulatory response that induces a decrease in O_2 concentrations once a certain threshold is reached during the accumulation of O_2 in the phase of high O_2 evolution in the morning. Such a switch in metabolism towards higher O_2 uptake would ultimately lead to transient O_2 undersaturation (Fig. 2a–c) within colonies, allowing for N_2 fixation to start during midday.

Impacts of colony formation

Colony formation resulted in pronounced microenvironments with O_2 undersaturation during a large part of the day, reaching nearly anoxic conditions in the center of some of the colonies (Fig. 2a–c). However, as colonies in this study were mostly net phototrophic over a period of several days (Fig. 1), the long phase of O_2 undersaturation must have been outbalanced by a *c.* 10 times shorter phase of strong O_2 supersaturation. Indeed, microsensor measurements revealed O_2 concentrations within colonies of up to 570 μmol l^{-1} (Figs S1, 2d). Even under air-equilibrated bulk conditions, O_2 concentrations within colonies therefore temporarily exceeded those supplied in the high O_2 treatment, where N_2 fixation was completely inhibited (Fig. 5a). However, this inhibitory effect of O_2 on N_2 fixation was reversible, as N_2 fixation rates could be increased by exposure to low O_2 concentrations (Fig. 5a), in line with previous studies showing recovery of nitrogenase after exposure to high O_2 (Zehr *et al.*, 1993). Hence, the lowered N_2 fixation in colonies compared with single trichomes is most likely not caused by damage to nitrogenase during the phase of high O_2 accumulation in the morning.

However, elevated O_2 concentrations may lead not only to inactivation or degradation of O_2-sensitive proteins such as nitrogenase, but also induce damage to other cellular components relevant for both N_2 fixation and C fixation, including lipids, proteins and DNA, through a concurrent increase in reactive oxygen species such as superoxide (e.g. Lesser, 2006). In line with this, high superoxide production by field-collected *Trichodesmium* colonies has been observed (Hansel *et al.*, 2016). Accumulation of O_2 and reactive oxygen species in the colony microenvironment may therefore increase the risk of oxidative stress in colonies compared with single trichomes and might be part of the reason why colonies showed lower N_2 and C fixation rates. The high rates of both gross O_2 evolution and O_2 uptake observed under elevated O_2 concentrations (Fig. 3) might place additional strain on the turnover of the photosynthetic machinery during the periods of elevated O_2 concentrations in colonies.

Moreover, the high rates of photosynthesis during the morning and evening (Fig. 1) may lead to a temporary depletion of carbon dioxide (CO_2) within the colony microenvironment. In line with this, a correlation of ^{13}C composition with colony size has been observed in field-collected *Trichodesmium* colonies, which may reflect cellular responses to CO_2 limitation in larger colonies (Tchernov & Lipschultz, 2008). In combination with the concurrently elevated O_2 concentrations, CO_2 depletion is likely to induce photorespiration and therefore lower C fixation rates. While CO_2 depletion can be partly compensated by carbon concentrating mechanisms (CCMs) such as the active uptake of bicarbonate (HCO_3^-), the elevated energy expenditure for CCMs poses an additional disadvantage for colonies compared with free-floating trichomes. Diffusion limitation in the colony microenvironment therefore involves several negative effects that may counteract the benefits of temporary O_2 depletion for N_2 fixation.

Our combined measurements of N_2 fixation rates and small-scale O_2 gradients contradict the hypothesis of colony formation as a mechanism to foster N_2 fixation by protecting nitrogenase from O_2 (Paerl & Bebout, 1988). Instead, we were able to demonstrate that O_2 undersaturation in the microenvironment (Fig. 2a–c) during the phase of typically highest nitrogenase activity (e.g. Berman-Frank *et al.*, 2001; Eichner *et al.*, 2014) did not result in elevated N_2 fixation rates in colonies (Fig. 5a). Consequently, we suggest that previous observations of higher or similar N_2 fixation rates in colonies compared with free-floating trichomes in the field (Saino & Hattori, 1982; Letelier & Karl, 1998) were not due to O_2 microenvironments, but due to other factors not included in our laboratory setting. These might include positive effects of colony formation on the nutritional status of *Trichodesmium* that are manifested only under nutrient-limited conditions in the field, such as enhanced dust dissolution (Rubin *et al.*, 2011) and more efficient interaction with bacterial associates producing siderophores and/or alkaline phosphatase (Chappell & Webb, 2010; Orcutt *et al.*, 2013; Lee *et al.*, 2017). By excluding these additional factors in our laboratory study under nutrient-replete conditions, we revealed that O_2 microenvironments *per se* did not lead to higher N_2 fixation rates in colonies compared with free-floating trichomes. In addition to microbial interactions and higher nutrient (P and Fe) availability, reduced grazing and efficient vertical movement along light and nutrient gradients (e.g. reviewed by Beardall *et al.*, 2009; Stal, 2017) may contribute to making colony formation a selective advantage in natural ecosystems.

Intracellular O_2 concentrations

Ultimately, nitrogenase activity is controlled by intracellular O_2 concentrations in the vicinity of the protein rather than extracellular O_2 conditions. On the cell surface of single trichomes, O_2 concentrations were never below 180 μmol l^{-1}. Hence, assuming that anoxic conditions are required in the vicinity of nitrogenase for it to function, cells must be able to establish a large gradient in O_2 concentrations across the cell wall. If cells are relatively impermeable, O_2 concentrations may differ strongly between neighboring cells in a trichome, depending on their specific metabolic activity. Our analysis of cell surface O_2 concentrations on a single-cell level revealed regions with reduced O_2 concentrations (Fig. 4b). While we cannot exclude that these are senescing or dividing cells, it is interesting to note that their occurrence and preferential localization in the center of single trichomes is also in line with the proposed concept of transiently or permanently nonphotosynthetic diazocytes (e.g. Lin *et al.*, 1998; Berman-Frank *et al.*, 2001).

To examine variation in intracellular O_2 in more detail, we modeled the relation between membrane permeability, intracellular O_2 concentrations and respiratory O_2 fluxes based on our data, using a model described in Damm *et al.* (2015; Notes S1). Previous studies examining the interplay of O_2 diffusion, consumption and N_2 fixation in *Trichodesmium* assumed either no or very low ($1–7 \times 10^{-1}$ m s^{-1}) diffusion resistance to O_2 for *Trichodesmium* cells (Staal *et al.*, 2003; Milligan *et al.*, 2007). Here, we chose a substantially different approach in that permeability of the cell wall was the ultimate model output. Assuming that nitrogenase can only function under locally anoxic conditions, we calculated the permeability that would be necessary to yield an O_2 concentration close to zero in the center of a diazocyte, based on cell dimensions and respiration rates measured by MIMS (Table 3). Since, strictly speaking, respiration cannot be sustained under anoxic conditions, the optimum intracellular O_2 concentration is most likely to be slightly above zero, and our model output represents a conservative estimate of the required diffusion resistance. As histological studies on *Trichodesmium* indicated that thylakoids are distributed relatively homogenously in the cytosol (Siddiqui *et al.*, 1992a) we assumed that there was uniform O_2 consumption throughout the cell.

Our model calculations revealed that single cells can achieve anoxic conditions in the center with a cell wall permeability for O_2 between 2.6×10^{-6} and 4.9×10^{-6} m s^{-1} if they perform dark respiration at the average rate observed in this study (homogenous respiration, Table 3). Based on a previous study demonstrating single-cell variation in cytochrome oxidase content that was correlated to nitrogenase content in *Trichodesmium thiebautii* (Bergman *et al.*, 1993), we also considered the effects of a six-fold higher respiration rate in diazocytes compared with vegetative cells, yielding somewhat higher permeability estimates between 1.6×10^{-5} m s^{-1} and 3.1×10^{-5} m s^{-1} (heterogeneous respiration, Table 3). These estimates exceed a previous one for

Table 3 Calculated permeability of the cell wall necessary to support anoxia in the interior of a *Trichodesmium* cell, based on measured rates of O_2 uptake (that is, dark respiration), extracellular O_2 concentrations in colonies and cell dimensions (average 5 μm length, 7 μm width).

Respiration distribution	External O_2 (μmol l^{-1})	Average O_2 uptake (fmol $cell^{-1}$ h^{-1})	Intensity of O_2 consumption (mol s^{-1} m^{-3})	Permeability for O_2 (m s^{-1})	Permeability for CO_2 (m s^{-1})
Homogeneous	329	608	1.49	4.6×10^{-6}	3.7×10^{-6}
Heterogeneous	329	3648	8.96	2.9×10^{-5}	2.3×10^{-5}
Homogeneous	187	194	0.48	2.6×10^{-6}	2.1×10^{-6}
Heterogeneous	187	1164	2.86	1.6×10^{-5}	1.3×10^{-5}
Homogeneous	101	198	0.49	4.9×10^{-6}	3.9×10^{-6}
Heterogeneous	101	1188	2.92	3.1×10^{-5}	2.4×10^{-5}

Scenarios with heterogeneous distribution of respiration assume a six-fold higher respiration rate in diazocytes compared to vegetative cells. Permeability for CO_2 was calculated from O_2 permeability using a conversion factor of 0.7961 according to Ramsing & Gundersen (1994). For further details on the model, please refer to Supporting Information Notes S1.

New Phytologist

Table 4 Calculated intracellular O_2 concentrations in *Trichodesmium* under net O_2 producing conditions (representative of early morning or evening), based on measured rates of O_2 production, extracellular O_2 concentrations in colonies, cell dimensions (5 μm length, 7 μm width), and membrane permeability calculated for diazocytes with an anoxic cell interior (Table 3).

Net O_2 production (fmol cell^{-1} h^{-1})	External O_2 concentration (μmol l^{-1})	Intensity of O_2 production (mol s^{-1} m^{-3})	Permeability for O_2 (m s^{-1})	Intracellular O_2 concentration (μmol l^{-1})
1031	329	2.53	4.6×10^{-6}	884
1031	187	2.53	2.6×10^{-6}	1166
1031	101	2.53	4.9×10^{-6}	623

Cell-specific O_2 production was calculated from a colony-specific measurement assuming 10 000 cells per colony. For further details on the model, please refer to Supporting Information Notes S1.

heterocysts (4×10^{-7} m s^{-1}; Walsby, 1985), in line with the fact that *Trichodesmium* cell walls lack the thick glycolipid layer that acts as a diffusion barrier in heterocysts. In contrast with eukaryotic cells, plasma membranes of *Trichodesmium* are surrounded by a peptidoglycan layer, which was also reported to be more pronounced than in other Gram-negative bacteria (Siddiqui *et al.*, 1992b), and can explain why our estimates for CO_2 permeability (calculated from O_2 permeability according to Ramsing & Gundersen, 1994; Table 3) are lower than estimates for diatoms (10^{-3} m s^{-1}; Hopkinson *et al.*, 2011). Carboxysomes, in turn, with their protein shell acting as a diffusion barrier to CO_2 (e.g. Rae *et al.*, 2013), are expected to have a lower permeability to CO_2 than the plasma membrane and cell wall. Accordingly, our estimates for CO_2 permeability exceeded previous estimates for the cyanobacterium *Synechococcus* that were based on measurements of cellular CO_2 efflux and therefore represent an integrated estimate for the cell wall and carboxysome (10^{-6}–10^{-7} m s^{-1}, Badger *et al.*, 1985; 10^{-8} m s^{-1}, Salon *et al.*, 1996).

As there are no indications for differences in membrane permeability between individual *Trichodesmium* cells, anoxic conditions in diazocytes must be accompanied by O_2 accumulation in photosynthesizing cells. Hence, while low permeability favors N_2 fixation in diazotrophic (nonphotosynthetic) cells, it also increases the risk for photorespiration and oxidative stress in vegetative (photosynthetic) cells. Applying membrane permeabilities between 2.6×10^{-6} and 4.9×10^{-6} m s^{-1} (calculated for diazocytes as described above; Table 3) and a photosynthesis rate of 1013 fmol cell^{-1} h^{-1} (based on an O_2 profile measured 10 h into the light period; Fig. 2d), we calculated intracellular O_2 concentrations representative for the net O_2 evolution phase in the morning/evening, yielding concentrations between 623 and 1166 μmol l^{-1} (Table 4). Intracellular O_2 concentrations can therefore differ strongly between single cells, depending on their instantaneous rates of photosynthesis and respiration. These rates may change significantly not only over the diel cycle but potentially also as cells switch between N_2-fixing and non-N_2-fixing states. The unexpected, transient nighttime increase in O_2 concentrations observed with microsensors within colonies (Fig. S1) and with optodes in the bulk medium in closed vials (Fig. 1b) furthermore suggests that intracellular O_2 dynamics may additionally be influenced by intracellular O_2 reservoirs and/or chemical binding of O_2, which should be targeted in future research.

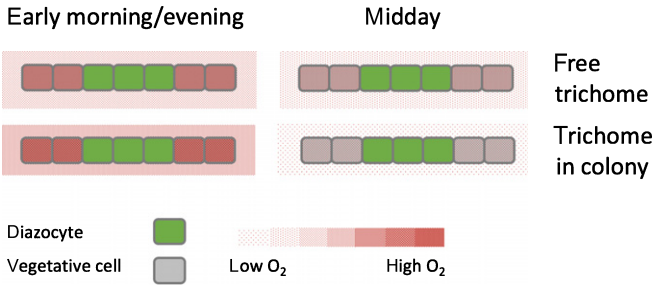

Fig. 6 Conceptual model of intra- and extracellular O_2 concentrations in *Trichodesmium* at different times of the day. Note that (nonphotosynthetic) diazocytes are always anoxic, while O_2 concentrations in vegetative (photosynthetic) cells vary with time of the day and morphology (colony vs free trichomes). Estimates are based on O_2 measurements (by microsensors and membrane inlet mass spectrometry (MIMS)) and model calculations, assuming the same photosynthesis rate and permeability for all cells. Red pattern in and around cells indicates O_2 concentration, grey and green backgrounds indicate vegetative cells and diazocytes, respectively.

Notably, our model calculations demonstrate that O_2 undersaturation on the cell surface is not a prerequisite for anoxic conditions in diazocytes. In fact, anoxic conditions could be achieved within nonphotosynthetic cells even under elevated ambient O_2 concentrations (Table 3). Colony formation as a means to form anoxic microenvironments is therefore not required, explaining why also single trichomes can fix N_2 at high rates (Fig. 5a). More generally, our model results highlight that due to the low permeability of the cell wall, intracellular O_2 concentrations in *Trichodesmium* are largely determined by cellular O_2 fluxes rather than extracellular microenvironments. Importantly, extracellular O_2 microenvironments can, however, indirectly affect intracellular conditions by inducing physiological responses of cellular O_2 fluxes to external O_2 concentrations (Fig. 3).

Conclusions

In summary, our measurements and model calculations demonstrate strong variations in O_2 concentrations in colony microenvironments and also indicate large variations within single cells (Fig. 6). These were induced by changes in the metabolic activity of *Trichodesmium* over the diel cycle, including high O_2 uptake during midday. Although colonies were undersaturated with O_2 during most of the day, this did not result in higher N_2 fixation

rates by colonies compared with single trichomes, potentially as the O_2 undersaturation over part of the day was accompanied by high extra- and intracellular O_2 concentrations during a short time window in the morning and evening. Based on our model calculations and high resolution microsensor measurements, we hypothesize that the diffusion barrier provided by the cell wall in combination with physiological heterogeneity between single cells allows for anoxic conditions within diazocytes, that is, respiring, nonphotosynthetic cells, under air-saturated bulk conditions (Fig. 6). Hence, O_2 undersaturation in colony microenvironments is not required to support N_2 fixation. Future research should therefore focus on the benefits of colony formation in *Trichodesmium* that outweigh the negative effects on C and N_2 fixation.

Acknowledgements

We thank the technical assistants in the microsensor group for construction of microsensors and Gabriele Klockgether, Philip Hach and Clarissa Karthäuser for help with EA-IRMS, ^{13}C-DIC and MIMS measurements. We also thank Laura Wischnewsky for phosphate measurements, as well as Tong Li and Dirk Koopmanns for helpful discussions. Funding was provided by the Alexander von Humboldt Foundation and the Max Planck Society.

Author contributions

ME, BR, WM and DdB designed the study, ME and SA performed the experiments and analyzed the data, ST performed the model calculations, ME, ST, BR, WM, SA, HP, MMMK and DdB discussed data interpretation and wrote the manuscript.

ORCID

Dirk de Beer https://orcid.org/0000-0001-5274-1781
Meri Eichner https://orcid.org/0000-0001-6106-7880
Wiebke Mohr https://orcid.org/0000-0002-1126-1455
Helle Ploug https://orcid.org/0000-0002-8989-245X
Björn Rost https://orcid.org/0000-0001-5452-5505
Silke Thoms https://orcid.org/0000-0002-0721-711X

References

Badger MR, Bassett M, Comins HN. 1985. A model for HCO_3^- accumulation and photosynthesis in the cyanobacterium *Synechococcus* sp. Theoretical predictions and experimental observations. *Plant Physiology* **77**: 465–471.

Beardall J, Allen D, Bragg J, Finkel Z, Flynn K, Quigg A, Rees TAV, Richardson A, Raven JA. 2009. Allometry and stoichiometry of unicellular, colonial and multicellular phytoplankton. *New Phytologist* **181**: 295–309.

Benavides M, Berthelot H, Duhamel S, Reimbault P, Bonnet S. 2017. Dissolved organic matter uptake by *Trichodesmium* in the Southwest Pacific. *Scientific Reports* **7**: 41315.

Bergman B, Carpenter EJ. 1991. Nitrogenase confined to randomly distributed trichomes in the marine cyanobacterium *Trichodesmium thiebautii*. *Journal of Phycology* **27**: 158–165.

Bergman B, Siddiqui PJA, Carpenter EJ, Peschek GA. 1993. Cytochrome oxidase: subcellular distribution and relationship to nitrogenase expression in the nonheterocystous marine cyanobacterium *Trichodesmium thiebautii*. *Applied and Environmental Microbiology* **59**: 3239–3244.

Berman-Frank I, Chen Y-B, Gao Y, Fennel K, Follows MJ, Milligan AJ, Falkowski PG. 2008. Feedbacks between the nitrogen, carbon and oxygen cycles. In: Capone DG, Bronk DA, Mulholland MR, Carpenter EJ, eds. *Nitrogen in the marine environment, 2nd edn*. Amsterdam, the Netherlands: Elsevier Inc., 1537–1563.

Berman-Frank I, Chen YB, Gerchman Y, Dismukes GC, Falkowski PG. 2005. Inhibition of nitrogenase by oxygen in marine cyanobacteria controls the global nitrogen and oxygen cycles. *Biogeosciences Discussion* **2**: 261–273.

Berman-Frank I, Lundgren P, Chen YB, Küpper H, Kolber Z, Bergman B, Falkowski P. 2001. Segregation of nitrogen fixation and oxygenic photosynthesis in the marine cyanobacterium *Trichodesmium*. *Science* **294**: 1534–1537.

Broecker WS, Peng TH. 1974. Gas exchange rates between air and sea. *Tellus* **26**: 21–35.

Burgess BK, Lowe DJ. 1996. Mechanism of molybdenum nitrogenase. *Chemical Reviews* **96**: 2983–3012.

Carpenter EJ, Chang J, Cottrell M, Schubauer J, Paerl HW, Bebout BM, Capone DG. 1990. Reevaluation of nitrogenase oxygen-protective mechanisms in the planktonic marine cyanobacterium *Trichodesmium*. *Marine Ecology Progress Series* **65**: 151–158.

Chappell PD, Webb EA. 2010. A molecular assessment of the iron stress response in the two phylogenetic clades of *Trichodesmium*. *Environmental Microbiology* **12**: 13–27.

Chen Y-B, Zehr JP, Mellon M. 1996. Growth and nitrogen fixation of the diazotrophic filamentous nonheterocystous cyanobacterium *Trichodesmium* sp. IMS 101 in defined media: evidence for a circadian rhythm. *Journal of Phycology* **32**: 916–923.

Damm E, Thoms S, Beszczynska-Möller A, Nöthig EM, Kattner G. 2015. Methane excess production in oxygen-rich polar water and a model of cellular conditions for this paradox. *Polar Science* **9**: 327–334.

Durner J, Böhm I, Knörzer OC, Böger P. 1996. Proteolytic degradation of dinitrogenase reductase from *Anabaena variabilis* (ATCC 29413) as a consequence of ATP depletion and impact of oxygen. *Journal of Bacteriology* **178**: 606–610.

Eichner MJ, Klawonn I, Wilson ST, Littmann S, Whitehouse MJ, Church MJ, Kuypers MMM, Karl DA, Ploug H. 2017. Chemical microenvironments and single-cell carbon and nitrogen uptake in field-collected colonies of *Trichodesmium* under different pCO_2. *ISME Journal* **11**: 1305–1317.

Eichner M, Kranz SA, Rost B. 2014. Combined effects of different CO_2 levels and N sources on the diazotrophic cyanobacterium *Trichodesmium*. *Physiologia Plantarum* **152**: 316–330.

Finzi-Hart JA, Pett-Ridge J, Weber PK, Popa R, Fallon SJ, Gunderson T, Capone DG. 2009. Fixation and fate of C and N in the cyanobacterium *Trichodesmium* using nanometer-scale secondary ion mass spectrometry. *Proceedings of the National Academy of Sciences, USA* **106**: 6345–6350.

Fock HP, Sültemeyer DF. 1989. O_2 evolution and uptake measurements in plant cells by mass spectrometer. In: Liskens HF, Jackson JF, eds. *Modern methods of plant analysis, vol. 9*. Heidelberg, Germany: Springer-Verlag, 3–18.

Fredriksson C, Bergman B. 1995. Nitrogenase quantity varies diurnally in a subset of cells within colonies of the non-heterocystous cyanobacteria *Trichodesmium* spp. *Microbiology* **141**: 2471–2478.

Gallon JR. 1992. Reconciling the incompatible: N_2 fixation and O_2. *New Phytologist* **122**: 571–609.

Großkopf T, LaRoche J. 2012. Direct and indirect costs of dinitrogen fixation in *Crocosphaera watsonii* WH8501 and possible implications for the nitrogen cycle. *Frontiers in Microbiology* **3**: 236.

Hansel CM, Buchwald C, Diaz JM, Ossolinski JE, Dyhrman ST, Van Mooy BAS, Polyviou D. 2016. Dynamics of extracellular superoxide production by *Trichodesmium* colonies from the Sargasso Sea. *Limnology and Oceanography* **61**: 1188–1200.

Hansen HP, Koroleff F. 1999. Determination of nutrients. In: Grasshoff K, Kremling K, Ehrhardt M, eds. *Methods of seawater analysis*. Weinheim, Germany: Wiley-VCH, 159–228.

Holm-Hansen O, Riemann B. 1978. Chlorophyll *a* determination: improvements in methodology. *Oikos* **30**: 438–447.

Hopkinson BM, Dupont CL, Allen AE, Morel FMM. 2011. Efficiency of the CO_2-concentrating mechanism of diatoms. *Proceedings of the National Academy of Sciences, USA* **108**: 3830–3837.

Kana TM. 1993. Rapid oxygen cycling in *Trichodesmium thiebautii*. *Limnology and Oceanography* **38**: 18–24.

Kranz SA, Levitan O, Richter KU, Prášil O, Berman-Frank I, Rost B. 2010. Combined effects of CO_2 and light on the N_2-fixing cyanobacterium *Trichodesmium* IMS101: physiological responses. *Plant Physiology* **154**: 334–345.

Kranz SA, Sültemeyer D, Richter K-U, Rost B. 2009. Carbon acquisition in *Trichodesmium*: the effect of pCO_2 and diurnal changes. *Limnology and Oceanography* **54**: 548–559.

Küpper H, Andresen E, Wiegert S, Šimek M, Leitenmaier B, Šetlík I. 2009. Reversible coupling of individual phycobiliprotein isoforms during state transitions in the cyanobacterium *Trichodesmium* analysed by single-cell fluorescence kinetic measurements. *Biochimica et Biophysica Acta (BBA)-Bioenergetics* **1787**: 155–167.

Küpper H, Ferimazov N, Šetlík I, Berman-Frank I. 2004. Traffic lights in *Trichodesmium*: regulation of photosynthesis for nitrogen fixation studied by chlorophyll fluorescence kinetic microscopy. *Plant Physiology* **135**: 2120–2133.

Lee MD, Walworth NG, McParland EL, Fu F-X, Mincer TJ, Levine NM, Hutchins DA, Webb EA. 2017. The *Trichodesmium* consortium: conserved heterotrophic co-occurrence and genomic signatures of potential interactions. *ISME Journal* **11**: 1813–1824.

Lesser MP. 2006. Oxidative stress in marine environments: biochemistry and physiological ecology. *Annual Reviews in Physiology* **68**: 253–278.

Letelier RM, Karl DM. 1998. *Trichodesmium* spp. physiology and nutrient fluxes in the North Pacific subtropical gyre. *Aquatic Microbial Ecology* **15**: 265–276.

Lin S, Henze S, Lundgren P, Bergman B, Carpenter EJ. 1998. Whole-cell immunolocalization of nitrogenase in marine diazotrophic cyanobacteria, *Trichodesmium* spp. *Applied and Environmental Microbiology* **64**: 3052–3058.

Milligan AJ, Berman-Frank I, Gerchman Y, Dismukes GC, Falkowski PG. 2007. Light-dependent oxygen consumption in nitrogen-fixing cyanobacteria plays a key role in nitrogenase protection. *Journal of Phycology* **43**: 845–852.

Ohki K, Fujita Y. 1988. Aerobic nitrogenase activity measured as acetylene reduction in the marine non-heterocystous cyanobacterium *Trichodesmium* spp. grown under artificial conditions. *Marine Biology* **98**: 111–114.

Ohki K, Taniuchi Y. 2009. Detection of nitrogenase in individual cells of a natural population of *Trichodesmium* using immunocytochemical methods for fluorescent cells. *Journal of Oceanography* **65**: 427–432.

Orcutt KM, Gundersen K, Ammerman JW. 2013. Intense ectoenzyme activities associated with *Trichodesmium* colonies in the Sargasso Sea. *Marine Ecology Progress Series* **478**: 101–113.

Paerl HW, Bebout BM. 1988. Direct measurement of O_2-depleted microzones in marine *Oscillatoria*: relation to N_2 fixation. *Science* **241**: 442–445.

Ploug H, Jørgensen BB. 1999. A net-jet flow system for mass transfer and microsensor studies of sinking aggregates. *Marine Ecology Progress Series* **176**: 279–290.

Ploug H, Kühl M, Buchholz-Cleven B, Jørgensen BB. 1997. Anoxic aggregates – an ephemeral phenomenon in the pelagic environment? *Aquatic Microbial Ecology* **13**: 285–294.

Ploug H, Passow U. 2007. Direct measurement of diffusivity within diatom aggregates containing transparent exopolymer particles. *Limnology and Oceanography* **52**: 1–6.

Rae BD, Long BM, Badger MR, Price GD. 2013. Functions, compositions, and evolution of the two types of carboxysomes: polyhedral microcompartments that facilitate CO_2 fixation in cyanobacteria and some proteobacteria. *Microbiology and Molecular Biology Reviews* **77**: 357–379.

Ramsing N, Gundersen J. 1994. *Seawater and Gases: Tabulated physical parameters of interest to people working with microsensors in marine systems, Techn Rep MPI Mar Microbiology Bremen.* [WWW document] URL http://www.unisense.com/files/PDF/Diverse/Seawater%20&%20Gases%20table.pdf [accessed 2 October 2018].

Rubin M, Berman-Frank I, Shaked Y. 2011. Dust-and mineral-iron utilization by the marine dinitrogen-fixer *Trichodesmium*. *Nature Geoscience* **4**: 529–534.

Saino T, Hattori A. 1982. Aerobic nitrogen fixation by the marine non-heterocystous cyanobacterium *Trichodesmium (Oscillatoria)* spp.: its protective mechanism against oxygen. *Marine Biology* **70**: 251–254.

Salon C, Mir NA, Canvin DT. 1996. Influx and efflux of inorganic carbon in *Synechococcus* UTEX625. *Plant, Cell & Environment* **19**: 247–259.

Siddiqui PJA, Carpenter EJ, Bergman B. 1992a. Ultrastructure and immunolocalization of phycobiliproteins and Ribulose-1,5-bisphosphate carboxylase/oxygenase in the marine cyanobacterium *Trichodesmium thiebautii*. *Journal of Phycology* **28**: 320–327.

Siddiqui PJ, Carpenter EJ, Bergman B. 1992b. *Trichodesmium*: ultrastructure and protein localization. In: Carpenter EJ, Capone DG, Rueter JG, eds. *Marine pelagic cyanobacteria:* Trichodesmium *and other diazotrophs*. Dordrecht, the Netherlands: Springer Netherlands, 9–28.

Spungin D, Berman-Frank I, Levitan O. 2014. *Trichodesmium*'s strategies to alleviate phosphorus limitation in the future acidified oceans. *Environmental Microbiology* **16**: 1935–1947.

Staal M, Meysman FJ, Stal LJ. 2003. Temperature excludes N_2-fixing heterocystous cyanobacteria in the tropical oceans. *Nature* **425**: 504–507.

Staal M, Rabouille S, Stal LJ. 2007. On the role of oxygen for nitrogen fixation in the marine cyanobacterium *Trichodesmium* sp. *Environmental Microbiology* **9**: 727–736.

Stal LJ. 2017. Gregarious cyanobacteria. *Environmental Microbiology* **19**: 2105–2109.

Tchernov D, Lipschultz F. 2008. Carbon isotopic composition of *Trichodesmium* spp. colonies off Bermuda: effects of colony mass and season. *Journal of Plankton Research* **30**: 21–31.

Tzubari Y, Magnezi L, Be'er A, Berman-Frank I. 2018. Iron and phosphorus deprivation induce sociality in the marine bloom-forming cyanobacterium *Trichodesmium*. *ISME Journal* **12**: 1682–1693.

Walsby AE. 1985. The permeability of heterocysts to the gases nitrogen and oxygen. *Proceedings of the Royal Society of London. Series B, Biological Sciences* **226**: 345–366.

Zehr JP, Wyman M, Miller V, Duguay L, Capone DG. 1993. Modification of the Fe protein of nitrogenase in natural populations of *Trichodesmium thiebautii*. *Applied and Environmental Microbiology* **59**: 669–676.

Supporting Information

Additional Supporting Information may be found online in the Supporting Information section at the end of the article:

Fig. S1 O_2 concentrations recorded within *Trichodesmium* colonies over several hours.

Notes S1 Calculation of the diffusion resistance to oxygen.

Please note: Wiley Blackwell are not responsible for the content or functionality of any Supporting Information supplied by the authors. Any queries (other than missing material) should be directed to the *New Phytologist* Central Office.